# INTERNATIONAL SOCIETY FOR SOIL MECHANICS AND GEOTECHNICAL ENGINEERING



This paper was downloaded from the Online Library of the International Society for Soil Mechanics and Geotechnical Engineering (ISSMGE). The library is available here:

# https://www.issmge.org/publications/online-library

This is an open-access database that archives thousands of papers published under the Auspices of the ISSMGE and maintained by the Innovation and Development Committee of ISSMGE.

The paper was published in the proceedings of the 7<sup>th</sup> International Young Geotechnical Engineers Conference and was edited by Brendan Scott. The conference was held from April 29<sup>th</sup> to May 1<sup>st</sup> 2022 in Sydney, Australia.

# Relating dynamic properties of gap-graded soils to the stress transmission in soil fabric

Relier les propriétés dynamiques des sols à écartement à la transmission des contraintes dans la structure du sol

Masahide Otsubo, Arian Ghaemi, Yang Li & Reiko Kuwano
Institute of Industrial Science (IIS), The University of Tokyo, Tokyo, Japan, otsubo@iis.u-tokyo.ac.jp

Troyee Tanu Dutta

Department of Civil Engineering, Monash University, Clayton, Victoria, Australia

ABSTRACT: Gap-graded soils, mixtures of finer and coarser soils, are used in geo-hydro structures. This research aims to relate dynamic properties of gap-graded soils to the participation of finer grains in the soil fabric. Laboratory element tests are conducted using mixtures of coarse and finer silica sands. Using triaxial apparatus equipped with planar piezoelectric transducers, elastic wave signals are recorded and analyzed to determine wave velocities, stiffness and maximum frequency propagated through the soil (lowpass frequency,  $f_{ip}$ ) at isotropic stresses. To quantify the stress-transmission through finer grains, complementary discrete element method simulations are performed using spheres with similar grain sizes. It was found that both stiffness and  $f_{ip}$  reduce at lower finer sand contents ( $F_s$ ), particularly when the size ratio is large, whereas  $f_{ip}$  increases sharply at higher  $F_s$ . The results suggest that quantifying  $f_{ip}$  can be used to characterize the fabric of gap-graded soil, whether finer grains contribute to the stress-transmission.

RÉSUMÉ: Les sols à granulométrie discontinue, mélange de sol fin et de sol grossier, sont courants en hydrogéologie. Ce travail a pour but d'étudier le lien entre les propriétés dynamiques d'un tel sol et la participation des granulats fins au "structure" du sol. Des essais en laboratoire sur des mélanges de sable de silice grossier et de sable de silice fin sont menés. À l'aide d'un appareil triaxial équipé de capteurs piézoélectriques, des signaux d'ondes élastiques sont analysés pour déterminer leur vitesse, la raideur du sol et la fréquence maximale de propagation des ondes dans le sol (filtre passe-bas de fréquence de coupure  $f_{ip}$ ) sous compression isotrope. Pour déterminer la transmission des efforts à travers les granulats fins, des calculs aux éléments finis sont menés en utilisant des sphères de taille équivalente à celle des granulats. Il a été constaté que la raideur du sol et  $f_{ip}$  diminuent pour des teneurs en sable fin  $(F_s)$  plus faibles, notamment lorsque le rapport de taille entre les granulats est grand, tandis que  $f_{ip}$  augmente fortement pour des  $F_s$  plus élevées. Les résultats suggèrent que la détermination de  $f_{ip}$  peut servir à déterminer la structure d'un sol à granulométrie discontinue, et si les granulats plus fins participent à la transmission des efforts.

KEYWORDS: elastic wave; gap-graded; fabric; geophysical testing; discrete element method.

# 1 INTRODUCTION

Gap-graded soils, mixtures of coarser and finer soils having a gap in their sizes, are occasionally used in geo-hydro structures such as earth-fill dams or embankments. Their erosion characteristics, e.g. suffusion, and mechanical properties, e.g. stiffness, strength or liquefaction resistance, have been investigated from a particle-scale perspective (e.g. Salgado et al. 2000; Rahman et al. 2008). It has been highlighted that participation of finer particles in the soil fabric is a key phenomenon to explain the complicated responses of gap-graded soils (Shire et al. 2014; Kawano et al. 2018). However, there is no established technique available to quantify the extent of the participation of finer particles in the soil fabric, in a non-destructive manner.

This contribution aims to relate dynamic properties of gap-graded soils to the participation of finer grains in the soil fabric. For this purpose, firstly, uniformly graded silica sands having various median particle sizes ( $D_{50}$ ) are tested to analyze their dynamic properties focusing on both the time-domain and frequency-domain responses. Discussions are extended to cover gap-graded silica sand mixtures by revisiting Dutta et al. (2021). Building on Otsubo et al. (2021), complementary discrete element method (DEM) simulations of gap-graded spherical particle assemblies are performed to quantify the contribution of finer particles to the fabric of gap-graded granular soils.

# 2 LABORATORY EXPERIMENT

# 2.1 Granular materials

Five sizes of uniformly graded silica sands having various  $D_{50}$  were used, termed as SS2, SS3, SS5, SS7 and SS8 (Fig. 1a). Since they were produced at the same site and sieved into different sizes, particle properties apart from their grain sizes were considered equivalent (Table 1). Gap-graded mixtures of SS3 and SS7 (Mix-37) having a median size ratio ( $R_d$ ) of 6.4 were also tested, where the finer sand content ( $F_s$ ) defined as the mass ratio of SS7 to the total was varied systematically (Fig. 1b).

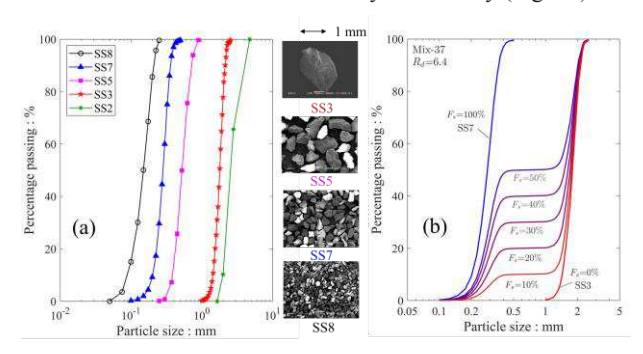


Figure 1. Particle size distribution (PSD) of tested materials. (a) Uniformly graded sandy soils (b) Gap-graded sandy soils (Mix-37).

Table 1. Material properties of the tested soil.

Material	$D_{50}$ [mm]	$C_u$	$G_s$	$e_{min}$	$e_{max}$
SS2	2.6	1.4	2.64	-	-
SS3	1.8	1.3	2.64	0.681	0.983
SS5	0.53	1.5	2.64	0.719	1.062
SS7	0.28	1.5	2.64	0.694	1.154
SS8	0.15	1.8	2.64	0.739	1.322

<sup>\*</sup> $C_u$ : Uniformity coefficient ( $D_{60}/D_{10}$ );  $G_s$ : specific gravity.

# 2.2 Laboratory element test preparation

Laboratory element test was conducted using a triaxial apparatus. The present test method broadly followed Dutta et al. (2021). Soil samples were prepared in a split cylindrical mold having 75mm in diameter and 150mm in height. Dry materials with approx. 1/5 of total mass are deposited into the mold using a funnel under zero-height drop condition to prepare a loose sample. This process was repeated approximately five times by minimizing material segregation. A similar consideration was made by Sarkar et al. (2020) for gap-graded materials. Effective stress (p') of 60kPa was applied to the sample using negative vacuum pressure, and then sample dimensions were measured directly. After performing non-destructive wave measurements under the isotropic stress state, a special technique described in Dutta et al. (2021) was adopted to continue the experiment. The initially loose specimen was densified at atmospheric pressure and then confined again at p'=60kPa with the denser sample. The sample density was increased by applying side blows to the entire height uniformly and carefully. Next, wave measurements were conducted after 1 hour of time duration at p'=60kPa.

#### 2.3 Shear wave measurements using DTs

Stress wave measurements using planar piezoelectric transducers have been utilized (e.g. Brignoli et al. 1996; Ismail & Rammah 2005; Dutta et al. 2019). A function generator and a bipolar amplifier were used to excite transmitter disk transducer (DT) in a shear mode (Fig. 2). A single-period sinusoidal pulse was input with a double amplitude of 140V. Transmitter and receiver DTs were placed inside the top cap and bottom pedestal, respectively, and their voltage signals were recorded using an oscilloscope (Fig. 2). Shear wave velocity ( $V_s$ ) was determined by L/T, where L and T are the length and the elapsed time of S-wave propagation. Following Yamashita et al. (2009) and Dutta et al. (2019), the peak-to-peak method was adopted to determine T using an input frequency ( $f_{in}$ ) of 7kHz. To characterize the frequency-domain responses particularly at higher frequencies, a broad range of  $f_{in}$  was used (even larger than 100kHz).

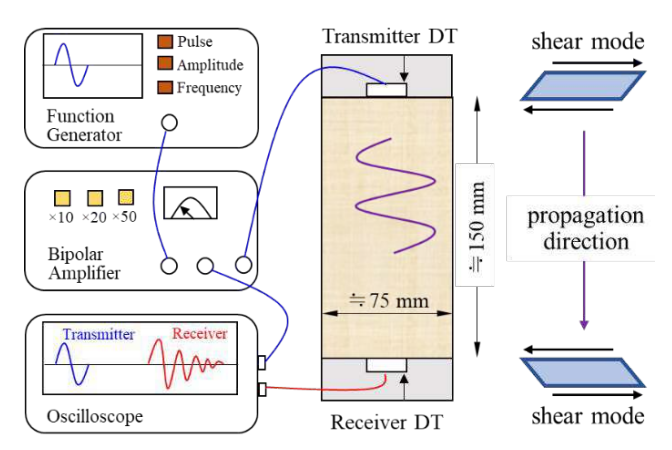


Figure 2. Schematic of testing condition and disk transducers (DTs).

#### B DISCRETE ELEMENT METHOD SIMULATION

# 3.1 Material and DEM sample preparation

A modified version of the open-source DEM code granular LAMMPS (Plimpton 1995) was used. Although the experiments used silica sands, spherical particles were considered in the DEM to understand the fundamentals of gap-graded soil behavior. Diameters of coarser and finer spherical particles were 1.2–2.2mm and 0.15–0.25mm, respectively, similar to SS3 and SS7, giving  $R_d$  of 8.8; this is slightly larger than  $R_d$  of 6.4 for Mix-37. The maximum number of particles in the simulations was about 2.3 million. Typical material properties for alkaline glass beads were used (Young's modulus=71.6GPa; Poisson's ratio=0.23;  $G_s$ =2.5). A simplified Hertz–Mindlin contact model with a Coulomb friction limit was used (Itasca 2007).

Samples were bounded by rigid walls and periodic boundaries in the longitudinal (Z-) and the horizontal (X- and Y-) directions, respectively (Fig. 3). A cloud of non-contacting particles was compressed using an in-house servo-control to p'=100kPa. The interparticle friction coefficients during isotropic compression ( $\mu$ ) of 0.01, 0.1 and 0.25 were selected to prepare dense, medium, and loose samples, respectively. The sample length ranged from 128mm to 159mm, whereas at least ten particles were placed in the horizontal directions. No gravitational force was applied in the simulations to prevent segregation of the coarser and finer particles. For more details of the sample preparation method, please refer to Otsubo et al. (2021).

#### 3.2 Wave measurements in DEM

After applying viscous damping to reach a static equilibrium, the  $\mu$  value was increased to 0.5 to ensure the elastic response of interparticle interaction during wave propagation. The damping was turned off during the subsequent wave propagation simulation. The entire transmitter wall was translated in the Xdirection (Fig. 3), and S-waves propagated towards the receiver wall in the Z-direction. Using periodic boundaries in the X- and Y-directions enabled to generate planar S-waves and prevent geometrical dissipation of propagating waves. The displacement of translation was controlled to be a single-period sinusoidal pulse with a double amplitude of 5nm. The same  $f_{in}$  values with the experiments were considered to determine  $V_s$  and the frequency-domain responses were analyzed. The resultant changes in shear stress on the transmitter and receiver walls were analyzed as analogue to the voltage signals in the experiments. For more details of the wave measurement approach, please refer to Otsubo et al. (2021).

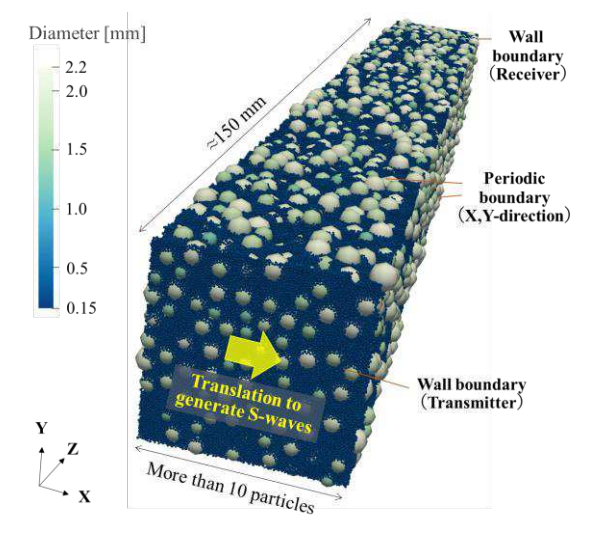


Figure 3. A representative medium-dense DEM sample with  $F_s$ =30%.

<sup>\*\*</sup> $e_{min}$ : minimum void ratio;  $e_{max}$ : maximum void ratio (JGS 0161, 2009).

# 4 LOWPASS THRESHOLD FREQUENCY

Granular materials exhibit lowpass filtering function when subjected to a broad range of frequencies (Santamarina et al. 2001; Mouraille & Luding 2008) as high-frequency contents cannot propagate through granular media. This threshold is defined as lowpass frequency ( $f_{lp}$ ) in this study.  $f_{lp}$  is a material property, and it increases with the density and confining stress (Otsubo et al. 2017). For uniformly graded sands, Dutta et al. (2019) found  $f_{lp}$  is larger for finer materials. This contribution provides more evidence on this aspect at a broader range of void ratio (e) and quantifies the  $f_{lp}$  for gap-graded soils.

# 5 UNIFORMLY GRADED SOIL

In general, for a given granular material, denser packing exhibits larger wave velocity (Hardin & Richart 1963), and the same trend was confirmed in the tested materials in this study. In the following discussion, the particle size-dependency of  $f_{lp}$  is investigated. Fig. 4a shows the time-domain responses of uniformly graded sands with various  $D_{50}$ , where SS3, SS5, SS7 and SS8 exhibit similar arrival time of S-waves and thus similar  $V_s$  (180±3 m/s) at slightly different e values. For the same test cases, Fig. 4b gives the variations of gain factor in the frequencydomain, i.e. amplitude ratio of the fast Fourier transforms (FFT) of receiver against transmitter (FFT<sub>rece</sub>/FFT<sub>tran</sub>). Adopting the approach in Dutta et al. (2019), fip was determined from Fig. 4b;  $f_{lp}$  is the highest frequency that exceeds a gain factor of  $2\times10^{-6}$ . This threshold may depend on test conditions and properties of DT and needs a careful validation. An apparent increase in  $f_{lp}$  is evident under the equivalent  $V_s$  as the  $D_{50}$  decreases.

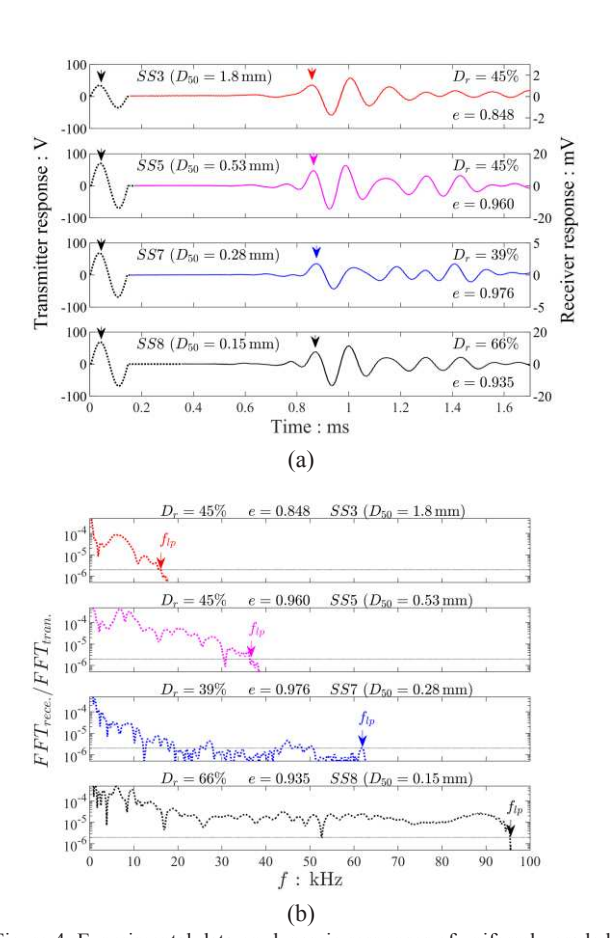


Figure 4. Experimental data on dynamic responses of uniformly graded sand samples. (a) Time-domain response (b) Frequency-domain response.

Fig. 5 illustrates the variation of  $f_{lp}$  with e for five sizes of sands. There is a linear variation between  $f_{lp}$  and e for each material, and its slope is higher for finer materials. For a given e, finer sands exhibit higher  $f_{lp}$  values. This grain size-dependent observation was compared with available data in Dutta et al. (2019). Fig.6a gives the relationship between  $D_{50}$  and  $f_{lp}$ normalized by the  $f_{lp}$  value equivalent to  $D_{50}$ =1mm of the same type (origin) of granular materials. To plot Fig. 6a, flp values at e=0.85 were interpolated for each material (extrapolated for SS2) from the linear variations in Fig. 5. Dutta et al. (2019) includes spherical glass beads, and spherical particle assemblies in DEM at different e. The current study adds more evidence of this finding even at different stress level. Besides, as Fig. 5 implies, a similar result can be obtained even when different *e* is selected. In contrast,  $V_s$  is not sensitive to  $D_{50}$  (Fig. 6b) where  $f_e$  is a void ratio function, having  $f_e = 1.74 - e$  as detailed in Dutta et al. (2019).

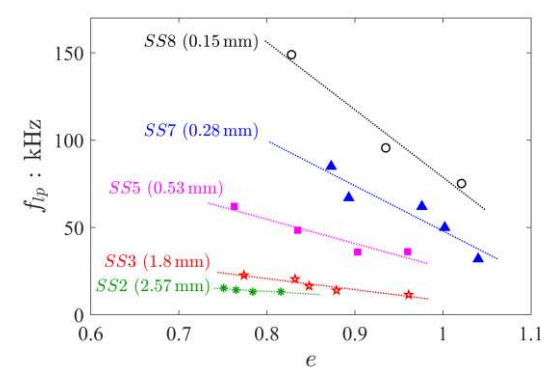


Figure 5. Experimental data on variation of lowpass frequency  $(f_{lp})$  with void ratio (e) for uniformly graded sand samples.

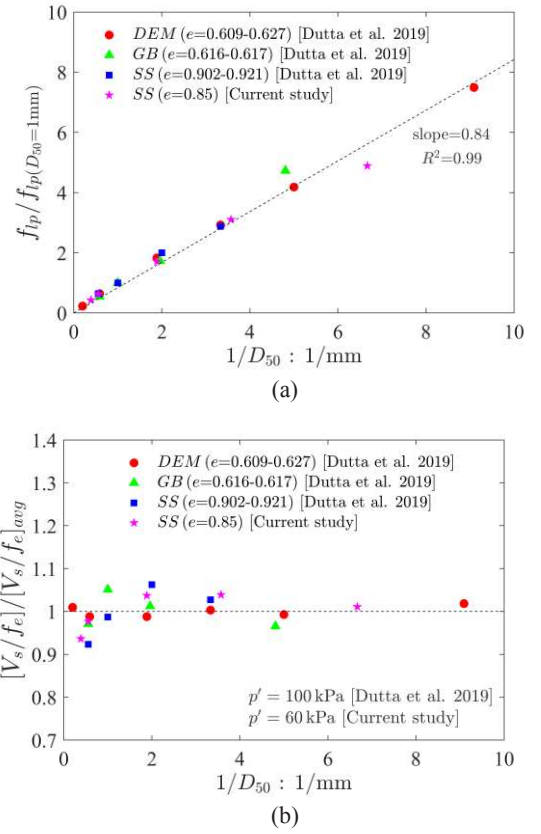


Figure 6. Sensitivity of grain-size on (a) Lowpass frequency  $(f_{lp})$  (b) Shear wave velocity  $(V_s)$  for uniformly graded sand samples.

# 6 GAP-GRADED SOIL

Sections 2.1 and 3.1 provide details of the gap-graded materials tested in the laboratory (Mix-37) and DEM, respectively. This section explores the packing characteristics and dynamic wave responses of the gap-graded materials. The experimental data and DEM data presented in Dutta et al. (2021) and Otsubo et al. (2021), respectively, were revisited and synthesized originally in this contribution to deepen the understanding of the mechanical response of gap-graded granular materials.

## 6.1 Packing characteristics

In the experiments, maximum void ratio ( $e_{max}$ ) and minimum void ratio ( $e_{min}$ ) were measured following the Japanese Geotechnical Society standard (JGS 0161, 2009) using a slightly larger mold (diameter: 80 mm, height: 60 mm) compared to the standard one. Fig. 7a shows the relationship between finer sand content ( $F_s$ ) and  $e_{max}$ ,  $e_{min}$  and void ratios equivalent to relative density ( $D_r$ ) of 70%, 50% and 30% where  $D_r$  is defined as ( $e_{max}-e$ )/( $e_{max}-e_{min}$ ). Fig. 7b shows variations of e for dense, medium, and loose DEM samples, as defined in Section 3.1. Spherical particle assemblies have limited ranges of attainable e, narrower than the experimental case (Fig. 7a). Otsubo et al. (2021) provides detailed packing analysis on the DEM samples. Liu et al. (2021) discusses packing characteristics of gap-graded granular materials of bimodal and trimodal PSD.

Fig. 7 depicts that e values of silica sand mixtures reach the minimal values at  $F_s$  of 35–40%, while spherical particle mixtures in DEM reach the minimal values at  $F_s$  of 25–30%. Sarkar et al. (2020) discusses grain shape effects on the packing of gap-graded soils, and Zuo & Baudet (2015); Dutta et al. (2021) review theoretical and empirical methods to predict the threshold  $F_s$  in terms of e.

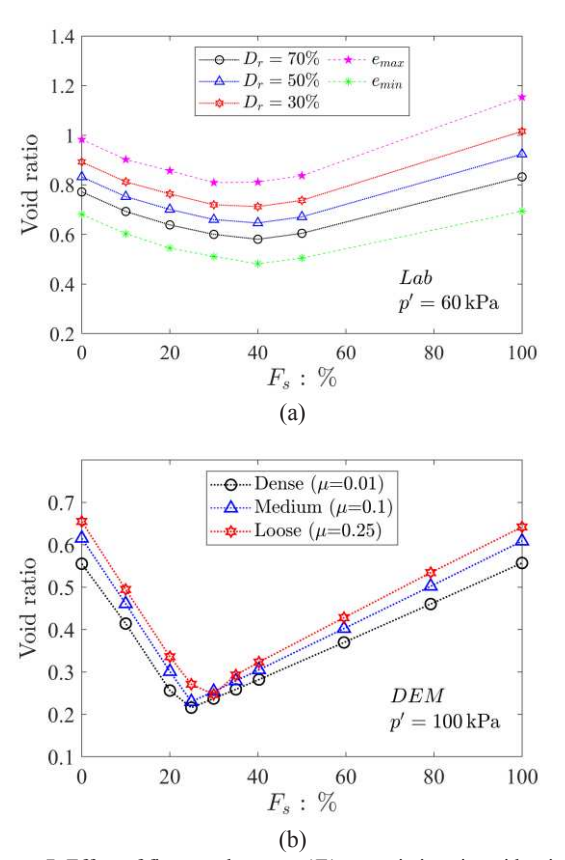


Figure 7. Effect of finer sand content ( $F_s$ ) on variations in void ratios (e) (a) Experimental data on silica sand mixtures (Mix-37) (b) DEM data on spherical particle mixtures.

# 6.2 Dynamic responses of gap-graded materials

For the dataset presented in Fig. 8, the variation of  $V_s$  with  $F_s$  is illustrated in Fig. 9. Referring to Dutta et al. (2021) the experimental data points equivalent to D<sub>r</sub>=70%, 50% and 30% were interpolated and used in the following discussion. For a given  $F_s$ ,  $V_s$  is larger for denser soil. For each density group,  $V_s$ declines at low  $F_s$  values in line with the literature (e.g. Salgado et al. 2000; Choo & Burns 2015; Goudarzy et al. 2016a; Yang & Liu 2016), while  $V_s$  turns to increase at  $F_s$  from 30% to 40%; this transition takes place slightly earlier for the denser case. DEM data show a similar trend (Fig. 8b) with the experimental result; however, the transition occurs at lower  $F_s$  than the experiment, which may be due to the difference in their particle shapes. The same reason may explain the trend that the initial decline in  $V_s$  at lower  $F_s$  is more obvious in the experimental data. The rise of  $V_s$ is attributed to the participation of finer particles in the soil fabric; however there is no evidence to support. The green shaded regions correspond to  $F_s$  from 25% to 45% for the experimental case (Fig. 8a), and 20% to 40% for the DEM case (Fig. 8b) to highlight the range for the transitional behavior.

Fig. 9 compares the variation in  $f_{lp}$  with  $F_s$  in a similar manner with Fig. 8. For a given  $F_s$ ,  $f_{lp}$  is larger for denser samples. For each density group,  $f_{lp}$  declines at low  $F_s$  values, and then turns to rise at the  $F_s$  similar to that for  $V_s$  (Fig. 8a). The transition in  $f_{lp}$  is more apparent than  $V_s$ , demonstrating clear density-dependency of the transitional response. The extent of rise in  $f_{lp}$  is also significant in the green shaded region compared with  $V_s$ .

A clear difference between  $f_{ip}$  and  $V_s$  is the difference in their values between  $F_s$ =0% and 100%, whose reason is confidently explained in Fig. 6. This gives a hypothesis that the increase in  $f_{ip}$  is a sign of active participation of finer particles in the soil fabric; this will be discussed in Section 7.

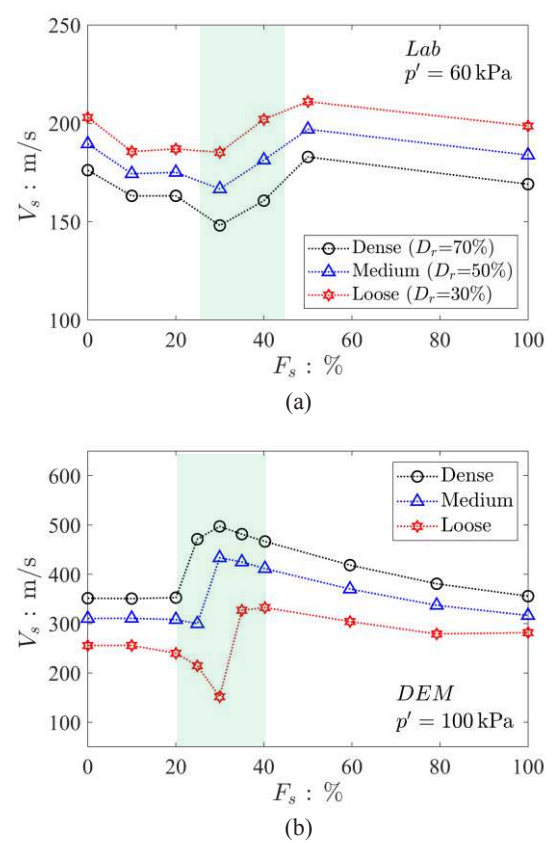


Figure 8. Variation in shear wave velocity ( $V_s$ ) with  $F_s$  (a) Experimental data on silica sand mixtures (Mix-37) (b) DEM data on spherical particle mixtures.

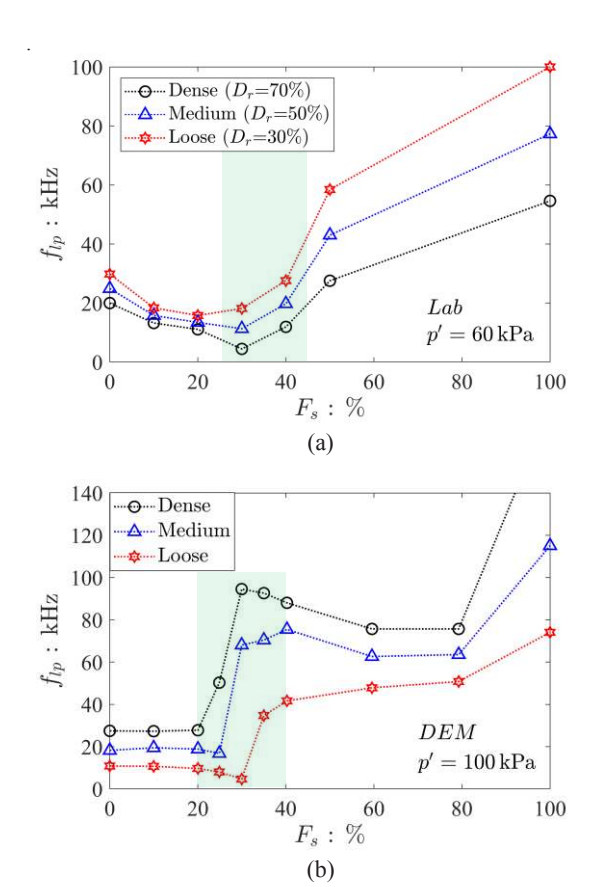


Figure 9. Variation in lowpass threshold frequency  $(f_{lp})$  with  $F_s$  (a) Experimental data on silica sand mixtures (Mix-37) (b) DEM data on spherical particle mixtures.

# 6.3 Limitations in comparison between experiment and DEM

This contribution compared the laboratory experimental data and DEM data in a qualitative manner realizing the following limitations in their comparison.

Firstly, experiments use silica sand mixtures (Mix-37), but DEM uses spherical particle mixtures where particle shapes are different. The later transitional response, i.e. at larger  $F_s$ , observed in the silica sand mixtures can be related to its angular particle shape; however, DEM study on gap-graded non-spherical particles requires huge computational costs.

Secondly, median particle size ratio ( $R_d$ ) is 6.4 for the experiment (Mix-37) but 8.8 for DEM case. For larger  $R_d$ , material segregation is inevitable in the experiment particularly for spherical particles like glass beads. Only limited experimental results are available using glass beads with a large  $R_d$  (e.g. Goudarzy et al. 2016a; Goudarzy et al. 2016b; Otsubo et al. 2019; Sarkar et al. 2020). On the other hand, the present DEM study ignores the gravity effect to avoid unexpected complexity.

Thirdly, the stress level at test was different between the experiment (p'=60kPa) and DEM (p'=100kPa). This directly influences the  $V_s$  and  $f_{lp}$  values. However for the purpose of qualitative comparison, Otsubo et al. (2021) reported similar trend between p'=50kPa and 100kPa based on gap-graded DEM samples with  $R_d=3.4$ .

Lastly, the ranges of density (or void ratio) were different between the experiment and DEM data, primarily due to the difference in particle shapes. More importantly, there is no established method to measure  $e_{min}$  and  $e_{max}$  in DEM to be comparable with the experimental data. This hinders comparisons under the equivalent relative density.

# 7 CONTRIBUTION OF FINES TO SOIL FABRIC

This section quantifies micromechanical properties of the DEM samples and relate the macroscopic mechanical responses (Figs. 8 and 9) to the participation of finer particles in the soil fabric. Particle coordination number (CN), i.e. number of contact points per particle, is illustrated in Fig. 10 for representative cores (cubic of 10mm in the middle part) of the DEM samples. At  $F_s$ =20%, most of finer particles exhibit CN close to 0, i.e. inactive, but coarser particles show mean CN of 6 and 5 for the dense and loose cases, respectively. At  $F_s$ =30%, the dense sample reveals a change in its fabric; finer particles are involved actively, and many coarser particles have CN>100. In contrast, the loose sample at  $F_s$ =30% gives a similar pattern with  $F_s$ =20% having slightly increased CN for coarser particles. At  $F_s$ =40%, the loose sample experiences a clear transition in its fabric where most finer particles are actively contributing to the soil fabric.

To quantify the stress transfer in the finer particles, a DEM-based approach presented in Shire et al. (2014) was considered. As detailed in Otsubo et al. (2021), an index of stress transfer via finer particles (excluding coarser-finer particle interactions) is depicted in Fig. 11 where larger value of the index indicates more contribution to the stress transfer, and its maximum value is about 1. It is at  $F_s$ =25%, 30% and 35% when finer particles start carrying measurable stress in the dense, medium, and loose cases, respectively. This result agrees with the observation in terms of CN (Fig. 10). Besides, this result supports the hypothesis made in Section 6.2; it is a sign of active participation of finer particles in the soil fabric when  $f_{lp}$  increases sharply.

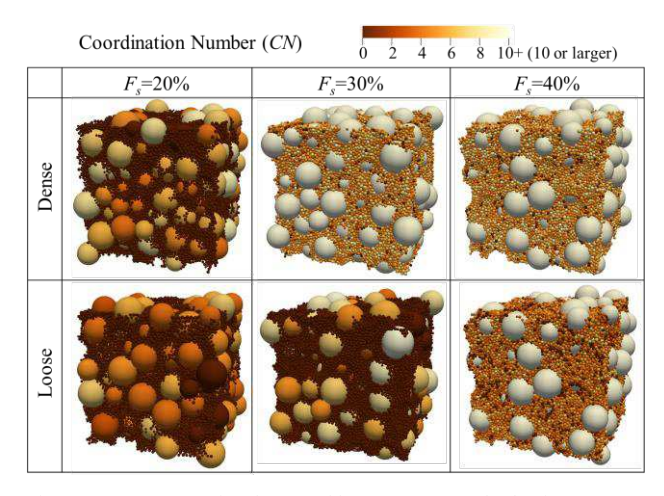


Figure 10. Representative dense and loose DEM samples having  $F_s$ =20%, 30% and 40%. Color indicates particle coordination number (CN).

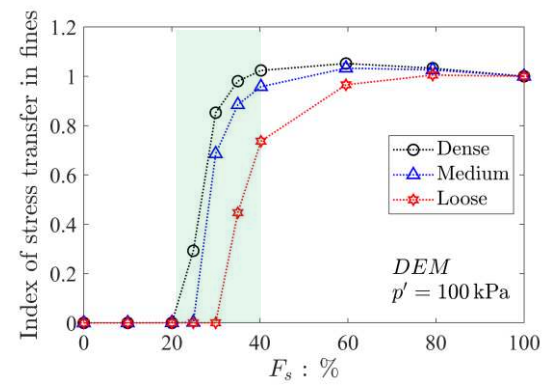


Figure 11. DEM results on index of stress transfer in finer particles with varying  $F_s$  (definition of this index is given in Otsubo et al. (2021)).

# 8 CONCLUSIONS

This contribution has explored the dynamic responses of granular materials focusing particularly on their frequency-domain responses. As a material property,  $f_{lp}$  values have been quantified using piezoelectric transducers for tested soil samples including uniformly graded soils and gap-graded cohesionless soils. The experimental condition is limited to the dry condition, specific sample preparation method and stress level of p'=60kPa. Complementary DEM simulations have been performed to understand the micro-scale responses of gap-graded soils, particularly for the particle-scale stress. Although a direct comparison between the experiments and DEM was not achieved in this study (refer to Section 6.3), the following conclusions can be drawn.

For uniformly graded soils (from experimental data)

- Both V<sub>s</sub> and f<sub>lp</sub> increase with increasing sample density. For a given density, f<sub>lp</sub> increases linearly with the inverse of D<sub>50</sub>, whereas V<sub>s</sub> is not sensitive to D<sub>50</sub>.
- The above-mentioned result can be applicable to samples of more spherical particles, confirmed by both experiments and DEM simulations in Dutta et al. (2019).
- From a dynamic wave survey, quantifying V<sub>s</sub> enables estimation of soil stiffness, while quantifying f<sub>ip</sub> potentially enables to estimate approximate particle sizes in the uniformly graded soil.

For gap-graded soils (from both experimental and DEM data)

- For the same host material (SS3 in the experiment), both  $V_s$  and  $f_{lp}$  increase with increasing sample density at a given  $F_s$ . For a given relative density or density type, there is nontrivial relationship between  $f_{lp}$  and  $F_s$  (also  $V_s$  and  $F_s$ ).
- Both  $V_s$  and  $f_{lp}$  decline at low  $F_s$  and turn to rise at higher  $F_s$ . The transition occurs earlier in denser samples and for spherical particle mixtures, e.g.  $30 \le F_s \le 40\%$  for the tested silica sand mixtures, and  $25 \le F_s \le 35\%$  for the tested spherical particles in DEM.
- fip is characterized by the particle size of dominant materials in gap-graded soils, i.e. either coarser or finer particles. fip is low when the soil fabric is dominated by coarser (host) particles, whereas fip is high when majority of finer particles are involved in the soil fabric.
- The above conclusion builds on the fact that finer-finer particle contacts allow high-frequency contents to propagate as confirmed confidently by the results for uniformly graded soils
- From a dynamic wave survey, quantifying V<sub>s</sub> enables of estimation of soil stiffness as widely understood. In addition, quantifying f<sub>Ip</sub> potentially enables to assess whether finer particles are actively contributing to the soil fabric or not.

# 9 ACKNOWLEDGEMENTS

This work was supported by JSPS KAKENHI Grant Number 19K15084. The simulations presented in this contribution were performed on Oakforest-PACS, The University of Tokyo. The authors thank Prof. Catherine O'Sullivan, Imperial College London, for her constructive advice on this research.

# 10 REFERENCES

- Brignoli E., Gotti M. & Stokoe K. 1996. Measurement of shear waves in laboratory specimens by means of piezoelectric transducers. *Geotechnical Testing Journal* 19 (4), 384-397.
- Choo H. & Burns S. 2015. Shear wave velocity of granular mixtures of silica particles as a function of finer fraction, size ratios and void ratios. *Granular Matter* 17 (5), 567-578.

- Dutta T., Otsubo M. & Kuwano R. 2021. Stress wave transmission and frequency-domain responses of gap-graded cohesionless soils. Soils and Foundations 61 (3), 857-873.
- Dutta T., Otsubo M., Kuwano R. & O'Sullivan C. 2019. Stress wave velocity in soils: Apparent grain-size effect and optimum input frequencies. Géotechnique Letters 9 (4), 340-347.
- Goudarzy M., König D. & Schanz T. 2016a. Small strain stiffness of granular materials containing fines. Soils and Foundations 56 (5), 756-764.
- Goudarzy M., Rahman M., König D. & Schanz T. 2016b. Influence of non-plastic fines content on maximum shear modulus of granular materials. Soils and Foundations 56 (6), 973-983.
- Hardin B.O. & Richart Jr.F.E. 1963. Elastic wave velocities in granular soils. *Journal of the Soil Mechanics and Foundations Division* 89 (1) (Proc. Paper 3407).
- Ismail, M. A. & Rammah, K. I. (2005). Shear-plate transducers as a possible alternative to bender elements for measuring G<sub>max</sub>. Géotechnique 55 (5), 403-407.
- Itasca (Itasca Consulting Group). 2007. PFC3D Version 4.0 user manual. Minneapolis, MN, USA: Itasca Consulting Group.
- Japanese Geotechnical Society, 2009. Test method for minimum and maximum densities of sands. Laboratory Testing Standards of Geomaterials, Vol. 1, JGS 0161.
- Kawano K. Shire T. & O'Sullivan C. 2018. Coupled particle-fluid simulations of the initiation of suffusion, *Soils and Foundations* 58 (4), 972-985.
- Liu D., O'Sullivan C. & Carraro J. 2021. Influence of particle size distribution on the proportion of stress-transmitting particles and implications for measures of soil state. *Journal of Geotechnical and Geoenvironmental Engineering*, 147 (3), 04020182.
- Mouraille O. & Luding S. 2008. Sound wave propagation in weakly polydisperse granular materials. *Ultrasonics* 48 (6-7), 498-505.
- Otsubo M., Dutta T.T., Durgalian M., Kuwano R. & O'Sullivan C. 2019. Particle-scale insight into transitional behaviour of gap-graded materials – small-strain stiffness and frequency response. In 7th International symposium on deformation characteristics of geomaterials (IS-Glasgow 2019) (eds A. Tarantino and E. Ibraim), E3S Web of Conferences vol. 92, article 14006.
- Otsubo M., Kuwano R. O'Sullivan C. & Shire T. 2021. Using geophysical data to quantify stress transmission in gap-graded granular materials. *Géotechnique* (Ahead of Print, 1-18). https://doi.org/10.1680/jgeot.19.P.334
- Otsubo M., O'Sullivan C. Hanley, K.J. & Sim W. 2017. Influence of packing density and stress on the dynamic response of granular materials. *Granular Matter* 19 (50), 1-18.
- Plimpton S. 1995. Fast parallel algorithms for short-range molecular dynamics. *Journal of Computational Physics* 117 (1), 1-19.
- Rahman M.M., Lo S.R. & Gnanendran C.T. 2008. On equivalent granular void ratio and steady state behaviour of loose sand with fines. *Canadian Geotechnical Journal* 45 (10), 1439-1456.
- Salgado R., Bandini P. & Karim A. 2000. Shear strength and stiffness of silty sand. *Journal of Geotechnical and Geoenvironmental* Engineering 126 (5), 451-462.
- Santamarina J.C., Klein K.A. & Fam M.A. 2001. Soils and waves: Particulate materials behavior, characterization and process monitoring, Wiley, Hoboken, New Jersey.
- Sarkar D., Goudarzy M., König D. & Wichtmann T. 2020. Influence of particle shape and size on the threshold fines content and the limit index void ratios of sands containing non-plastic fines. *Soils and Foundations* 60 (3), 621-633.
- Shire T., O'Sullivan C., Hanley K.J. & Fannin R.J. 2014. Fabric and effective stress distribution in internally unstable soils. *Journal of Geotechnical and Geoenvironmental Engineering* 140 (12), 04014072.
- Yamashita S., Kawaguchi T., Nakata Y., Mikami T., Fujiwara T. & Shibuya S. 2009. Interpretation of international parallel test on the measurement of  $G_{max}$  using bender elements. *Soils and Foundations* 49 (4), 631-650.
- Yang J. & Liu X. 2016. Shear wave velocity and stiffness of sand: the role of non-plastic fine. *Géotechnique* 66 (6), 500-514.
- Zuo L. & Baudet B.A. 2015. Determination of the transitional fines content of sand-non plastic fines mixtures. Soils and Foundations 55 (1), 213-219.